

Article

High-Value Recovery of the Iron via Solvent Extraction from Waste Nickel-Cadmium Battery Sulfuric Acid Leachate Using Saponified D2EHPA

Lei Zhou ¹, Yongqing Zhang ^{1,2,3,*}, Lijin Zhang ¹, Xuefeng Wu ¹, Ran Jiang ⁴ and Lu Wang ¹

¹ School of Environment and Energy, Guangdong Provincial Key Laboratory of Atmospheric Environment and Pollution Control, South China University of Technology, Guangzhou 510640, China; 202021048347@mail.scut.edu.cn (L.Z.); 202120147871@mail.scut.edu.cn (L.Z.); 202121049198@mail.scut.edu.cn (X.W.); 202020147168@mail.scut.edu.cn (L.W.)

² The Key Lab of Pollution Control and Ecosystem Restoration in Industry Clusters, Ministry of Education, Guangzhou 510006, China

³ State Key Laboratory of Pulp and Paper, South China University of Technology, Guangzhou 510006, China

⁴ The Pearl River Hydraulic Research Institute, Pearl River Water Resources Commission of the Ministry of Water Resources, Guangzhou 510640, China; ranjiangniuniu@163.com

* Correspondence: zhangyq@scut.edu.cn; Tel.: +86-13434389968; Fax: +86-20-39380508

Abstract: A significant amount of iron from the waste nickel-cadmium (Ni-Cd) battery sulfuric acid leachate seriously hinders the separation and recovery of nickel and cadmium. Therefore, an efficient and economical way to remove iron from this leachate is desired. This paper demonstrated the efficient iron extraction from a simulated Ni-Cd battery sulfuric acid leachate with saponified Di (2-ethylhexyl) phosphoric acid (D2EHPA). The iron-loaded D2EHPA was then stripped with oxalic acid and the iron was recovered in the form of iron oxalate. This process realizes the efficient separation and high-value recovery of iron. The results showed that the saponification of the D2EHPA greatly promoted the extraction of iron from the Ni-Cd battery sulfuric acid leachate. Under suitable conditions, the iron's single-stage extraction rate was more than 95%, and the iron's single-stage stripping rate was more than 85%. Moreover, the iron's extraction rate was more than 99% after two theoretical extraction stages, and the stripping rate was 95.6% after two theoretical stripping stages. The slope analysis determines that five molecules of D2EHPA were combined with one molecule of Fe³⁺ in the extraction process. The FT-IR analysis shows that the extraction mechanism of Fe³⁺ using the saponified D2EHPA is a cation exchange. These results can help guide the industrial separation and recovery of iron from the waste Ni-Cd battery sulfuric acid leachate.

Keywords: waste nickel-cadmium batteries; saponified D2EHPA; extraction of iron; iron oxalate

Citation: Zhou, L.; Zhang, Y.; Zhang, L.; Wu, X.; Jiang, R.; Wang, L. High-Value Recovery of the Iron via Solvent Extraction from Waste Nickel-Cadmium Battery Sulfuric Acid Leachate Using Saponified D2EHPA. *Separations* **2023**, *10*, 251. <https://doi.org/10.3390/separations10040251>

Academic Editor: Sascha Nowak

Received: 20 March 2023

Revised: 8 April 2023

Accepted: 11 April 2023

Published: 12 April 2023



Copyright: © 2023 by the authors. Licensee MDPI, Basel, Switzerland. This article is an open access article distributed under the terms and conditions of the Creative Commons Attribution (CC BY) license (<https://creativecommons.org/licenses/by/4.0/>).

1. Introduction

Nickel-Cadmium (Ni-Cd) batteries are widely used in rail transit, aircraft, and power grid energy storage due to their stable performance, long life, and fast discharging capability [1,2]. However, the carcinogenic metals cadmium and nickel make these batteries hazardous wastes without the proper treatment and disposal, which poses a threat to human health and the environment [3]. Recently, many researchers believe that the large amounts of nickel and cadmium contained in waste Ni-Cd batteries are a high-value resource [4,5]. As such, using the appropriate methods for their separation and recycling can reduce environmental pollution and provide significant economic benefits.

The commonly used recycling technologies for nickel-cadmium batteries mainly include pyrometallurgical treatment and hydrometallurgical treatment [6]. Pyrometallurgical treatment is a mature waste battery recycling process, but it has drawbacks of high energy consumption, toxic gas emission, and low-value products [1]. The

hydrometallurgical process is considered to be a more sustainable battery waste recycling route due to its good separation effect, high-value products, and lower waste emission [5].

The acid leachate produced in the hydrometallurgical process, commonly used in recycling spent Ni-Cd batteries, generally contains metals such as nickel, cadmium, cobalt, and iron [7]. The presence of iron seriously impacts the recycling of nickel, cadmium, and cobalt [8]. At present, the commonly used iron removal processes include iron-vanadium precipitation, extraction, and ion exchange [9]. Precipitation has significant advantages in removing low concentrations of iron from the acid leachate. However, it also creates difficulties in the solid-liquid separation and the loss of other metals through co-precipitation [10]. Ion exchange selectively removes most of the iron, but the expensive operating costs limit its potential application [11]. Solvent extraction for iron removal has the benefits of good separation, high product purity, and automation. These benefits have attracted the attention of many researchers [12].

Di (2-ethylhexyl) phosphoric acid (D2EHPA) [13], 2-ethylhexyl phosphonic acid mono-2-ethylhexyl ester (P507) [14], tertiary amine (N235) [15], tributyl phosphate (TBP) [16], and bis (2,4,4-tri-methylpentyl) (Cyanex 272) [17] have been used as solvents to remove iron from various acidic leachates. Hu et al. studied iron's selectivity relative to other impurities while removing it from a highly concentrated chloride solution using D2EHPA [13]. Wang et al. studied the optimal conditions for the P507 extraction of iron from coal fly ash leachate and found that P507's iron extraction mechanism was ion exchange [14]. Sun et al. proposed a synergistic extractant consisting of D2EHPA and N235 to extract iron from an aluminum solution. The single-stage iron extraction rate was more than 97%, and iron's stripping efficiency was greater than 99% with 1 mol/L sulfuric acid [15]. Yi et al. investigated iron's extraction mechanism from Ni-Co-Fe chloride solutions using TBP and concluded that the iron complexes formed with TBP and 2-octanol were $[H_2FeCl_4 \cdot 2 TBP]$ and $[H_2FeCl_4 \cdot 5 (2-octanol)]$ [16]. Pav'ón et al. used Cyanex 572 (a PC88A/Cyanex 272 mixture) to extract iron from phosphoric acid with an extraction rate of 98.1% and 2 mol/L HCl almost completely stripped iron [17]. Considering the economic cost and readily available raw material, D2EHPA is still the better choice for the separation of low-value metal iron via large-scale industrial extraction. In recent years, there have been several reports investigating the effects of saponification on metal extraction [18,19], but only a few studies have shown the effects of saponification on iron extraction using D2EHPA. Meanwhile, the effects of saponified D2EHPA on the extraction and separation of higher Fe^{3+} concentrations (~12 g/L) from sulfuric acid leachates that also contain high concentrations of Ni^{2+} (~56 g/L) and Cd^{2+} (~23 g/L) are also less well known.

In this work, saponified D2EHPA is used to extract iron from a simulated spent Ni-Cd battery sulfuric acid leachate. This is followed by stripping the extract with oxalic acid to obtain an iron oxalate solution as a high-value product. This method achieves the highly efficient separation of iron from the simulated Ni-Cd battery leachate and the high-value recycling of iron. The effects of saponification rate, extractant concentration, extraction time, extraction temperature, stripping agent concentration (oxalic acid), stripping time, and stripping temperature were explored. Slope analysis was used to study the mechanism of extraction. Fourier transform infrared spectra (FT-IR) analysis was used to characterize the organic phase during the saponification, extraction, and stripping process. This allows one to elucidate the mechanisms of saponification, extraction, and stripping.

2. Materials and Methods

2.1. Materials and Solutions

The extractant D2EHPA and diluent sulfonated kerosene were purchased from Zhengzhou Deyuan Fine Chemicals Co., Ltd. Both reagents were used without further purification. Analytical grade $Fe_2(SO_4)_3 \cdot xH_2O$, $CdSO_4 \cdot 3/8H_2O$, $NiSO_4 \cdot 6H_2O$, and $CoSO_4 \cdot 7H_2O$ were purchased from Shanghai Aladdin Chemistry Inc., Shanghai, China, and used as is.

The concentration of D2EHPA was 1 mol/L, except for the extractant concentration experiment. The D2EHPA was saponified with 10 mol/L sodium hydroxide, and the saponification rate was 70%. Deionized water used to make the solutions was obtained from a Milli-Q system. A spent Ni-Cd battery sulfuric acid leachate was simulated by dissolving $\text{Fe}_2(\text{SO}_4)_3 \cdot x\text{H}_2\text{O}$, $\text{CdSO}_4 \cdot 3/8\text{H}_2\text{O}$, $\text{NiSO}_4 \cdot 6\text{H}_2\text{O}$, and $\text{CoSO}_4 \cdot 7\text{H}_2\text{O}$ in 0.05 mol/L H_2SO_4 . The metal ion content in the simulated leachate is provided in Table 1.

Table 1. The major metal ion concentrations in simulated leachate.

Elements	Content (g/L)
Fe	12.25
Ni	56.30
Cd	23.28
Co	0.52

2.2. Experimental Procedure

The extraction experiments were conducted in a separatory funnel by shaking the extractant and simulated leachate mixtures with an oscillation rate of 200 rpm. After resting and phase separation, the aqueous raffinate layer was removed from the bottom of the separatory funnel. Stripping experiments were similar to the extraction, where the organic phase was iron-loaded D2EHPA, and the aqueous phase was the stripping agent oxalic acid.

2.3. Analytical Method

The metal ion concentration in the raffinate was determined by an atomic absorption spectrometer (AAS, AA6880F, Shimadzu, Japan). The metal ion content in the extractant was then calculated by mass balance. The pH was measured using a pH meter (PHS-3C, INESA Scientific Instrument Co., Ltd., Shanghai, China). The Fourier transform infrared spectra (ATR-FTIR, Thermo Scientific Nicolet iN10) were recorded from 4000–400 cm^{-1} .

The extraction rate (E), distribution ratio (D), separation coefficient (β), and stripping rate (S) were calculated using Equations (1)–(5):

$$E = \left(\frac{C_{a,0} - C_{a,1}}{C_{a,0}} \right) \times 100\% \tag{1}$$

$$C_{org,1} = \frac{C_{a,0} - C_{a,1}}{R_1} \tag{2}$$

$$D = \frac{C_{org,1}}{C_{a,1}} \tag{3}$$

$$\beta_{Fe/M} = \frac{D_{Fe}}{D_M} \tag{4}$$

$$S = \left(\frac{C_{a,2}}{R_2 \times C_{org,1}} \right) \times 100\% \tag{5}$$

where $C_{a,0}$ is the metal ion concentration in the simulated leachate, $C_{a,1}$ is the metal ion concentration in the raffinate solution, R_1 is the phase ratio on the extraction, $C_{a,2}$ is the metal ion concentration in the strip liquor, and R_2 is the phase ratio on the stripping.

3. Results and Discussion

3.1. Extraction Performance of Fe^{3+}

3.1.1. Extraction of Fe^{3+} from the Waste Ni-Cd Battery Sulfuric Acid Leachate

The major metal ions in the simulated waste Ni-Cd battery sulfuric acid leachate include Fe^{3+} , Ni^{2+} , Cd^{2+} , and Co^{2+} , with concentrations of 12.25 g/L, 56.30 g/L, 23.28 g/L, and

0.52 g/L, respectively. The concentrations of Cd^{2+} and Ni^{2+} are much higher than that in previous works [13,16], which makes it difficult to separate Fe^{3+} from the simulated leachate.

Saponified D2EHPA (saponification rate of 70%, 1 mol/L) was used to extract iron from the simulated leachate. As is shown in Figure 1, the extraction rate of Fe^{3+} was more than 95%, and the extraction rates of Cd^{2+} , Ni^{2+} , and Co^{2+} were all below 5%. The separation coefficients of $\beta_{\text{Fe}/\text{Cd}}$, $\beta_{\text{Fe}/\text{Ni}}$, and $\beta_{\text{Fe}/\text{Co}}$ were 423, 476, and 394, respectively. This data indicates that the saponified D2EHPA is able to selectively extract Fe^{3+} from a sulfate solution with a high concentration of Cd^{2+} and Ni^{2+} .

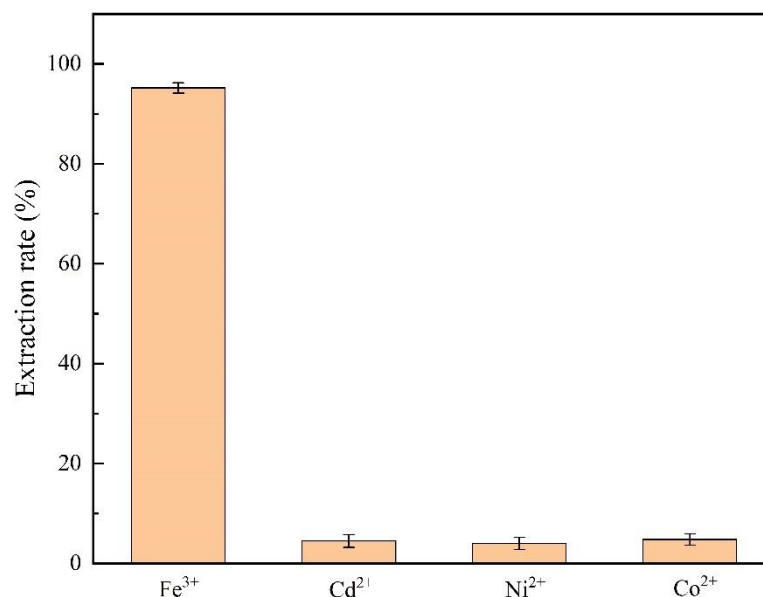


Figure 1. Saponified D2EHPA metal ion extraction rate from synthetic leachate under the conditions: room temperature (298 K), $[\text{D2EHPA}] = 1 \text{ mol/L}$, initial $[\text{Fe}^{3+}] = 12.25 \text{ g/L}$, extraction time = 20 min, saponification rate = 70%, initial pH = 1.00, and phase ratio = 1:1.

3.1.2. Effects of Saponification Rate of D2EHPA

When untreated D2EHPA was used to extract the metal ions, large amounts of hydrogen ions were transferred from the organic phase into the aqueous phase, inhibiting the extraction of iron [20]. To determine the optimum saponification rate, the rate was varied from 0% to 100%, while the extraction was carried out under an extraction temperature of 298 K, D2EHPA concentration of 1 mol/L, initial pH of 1.00, initial concentration of Fe^{3+} of 12.25 g/L, and extraction time of 20 min.

Figure 2 shows the iron extraction rate is only 65.12% with untreated D2EHPA. Increasing the saponification rate significantly increases the extraction rate. When the saponification rate was 70%, the iron extraction rate exceeded 95%, and the Cd, Co, and Ni extraction rates were all below 5%. As the saponification rate was further increased to 80%, 90%, and 100%, the iron extraction rate increased slightly, and the Cd and Ni extraction rates increased to over 10%, which impacted the purity of the obtained iron product. In order to maximize the iron extraction rate and reduce the co-extraction of cadmium, nickel, and cobalt, 70% saponified D2EHPA was used in subsequent experiments.

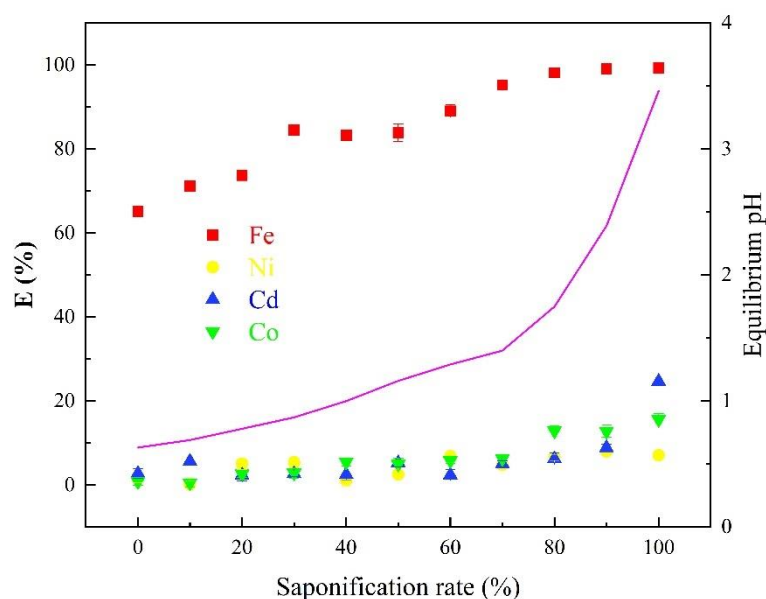


Figure 2. Effects of D2EHPA saponification rate on the extraction under the conditions: room temperature (298 K), [D2EHPA] = 1 mol/L, initial $[Fe^{3+}] = 12.25$ g/L, extraction time = 20 min, initial pH = 1.00, and phase ratio = 1:1.

The thermodynamic equilibrium species of iron was calculated by Visual MINTEQ with a pH varying from 0.00 to 6.00. Figure 3 shows that $[FeSO_4]^+$ was the main iron species at a pH from 0 to 4. The amounts of $[FeSO_4]^+$ increased with pH from 0 to 1.75 and decreased with the higher pH value. Meanwhile, $[Fe(OH)^{2+}]$, $[Fe_2(OH)_2]^{+4}$, and $[Fe_3(OH)_4]^{+5}$ emerged at a pH of 2.50, indicating that iron began to hydrolyze[14]. The purple line in Figure 2 shows the extract pH increasing as the saponification rate increases. With 70% saponified D2EHPA, the equilibrium pH was 1.40, while $[FeSO_4]^+$ was the major iron species from Figure 3. The results show that the iron was extracted by 70% saponified D2EHPA with a high extraction rate.

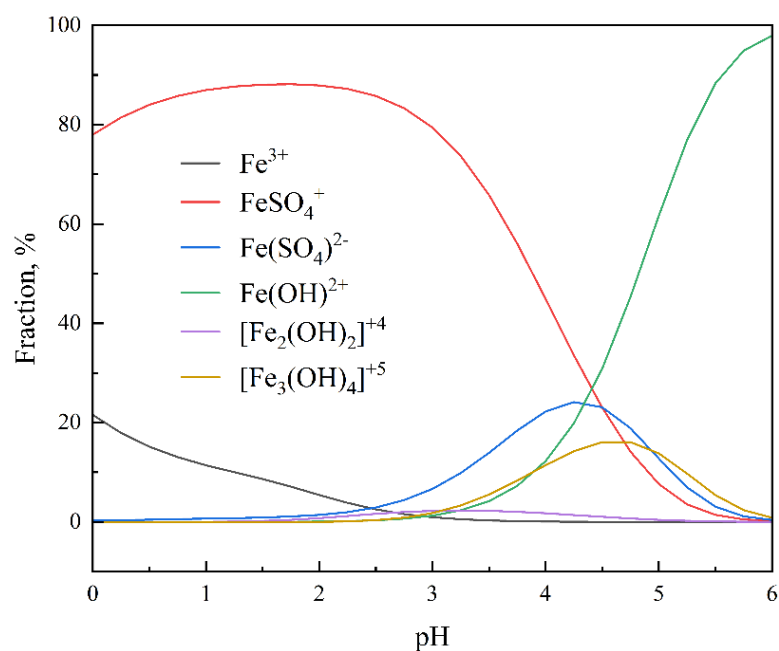


Figure 3. Iron species distribution in the leachate at various pHs under the conditions: $[Fe^{3+}] = 12.25$ g/L, $[Cd^{2+}] = 23.28$ g/L, $[Ni^{2+}] = 56.30$ g/L, and $[Co^{2+}] = 0.52$ g/L.

3.1.3. Effects of Extraction Time

Figure 4 shows the effect of extraction time varying from 5 min to 60 min on iron extractions, where other conditions were an extraction temperature of 298 K, D2EHPA concentration of 1 mol/L, saponification rate of 70%, initial pH of 1.00, initial concentration of Fe³⁺ of 12.25 g/L, and phase ratio of 1:1. The Fe³⁺ extraction rate increased with increasing extraction times and reached a peak of ~95% at 10 min. The results suggest that the iron extraction under these conditions was completed in 10 min. In order to ensure maximum iron extraction, a 20 min extraction time was used in the other experiments.

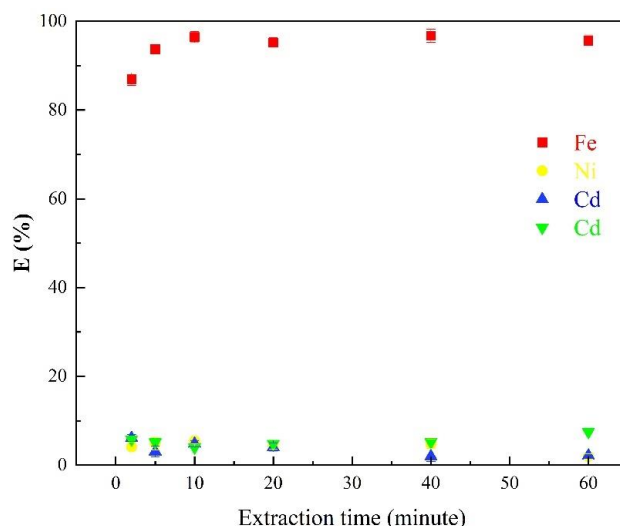


Figure 4. Effects of extraction time under the conditions: room temperature (298 K), [D2EHPA] = 1 mol/L, initial [Fe³⁺] = 12.25 g/L, saponification rate = 70%, initial pH = 1.00, and phase ratio = 1:1.

3.1.4. Effects of Temperature on the Extraction

In this section, the effects of the extraction temperature (298 K–323 K) on the extraction of Fe³⁺ from the synthetic sulfuric acid leachate were studied under the D2EHPA concentration of 1 mol/L, saponification rate of 70%, initial concentration of Fe³⁺ of 12.25 g/L, extraction time of 20 min, initial pH of 1.00, phase ratio of 1:1. As is shown in Figure 5, the extraction rate of Fe³⁺ was basically constant with the increase of the extraction temperature. It can be inferred that extraction temperature has a slight effect on iron extraction. In order to simplify the experimental operations and reduce energy use further, extraction experiments were carried out at 298 K.

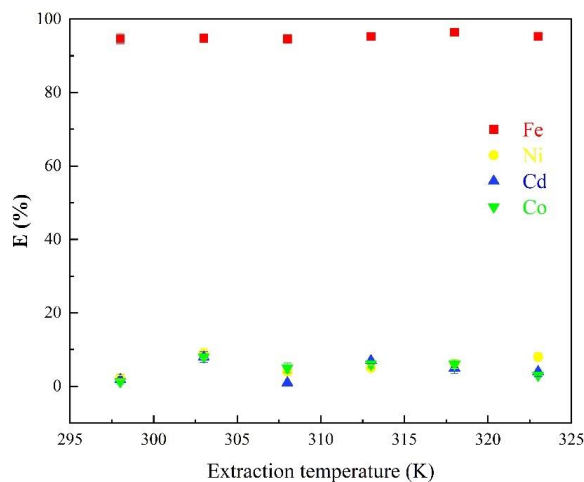


Figure 5. Effects of extraction temperature under the conditions: [D2EHPA] = 1 mol/L, saponification rate = 70%, initial [Fe³⁺] = 12.25 g/L, extraction time = 20 min, initial pH = 1.00, and phase ratio = 1:1.

3.1.5. Effects of D2EHPA Concentration on the Extraction

Saponified D2EHPA with concentrations varying from 0.2 mol/L to 1.3 mol/L were used to extract Fe^{3+} from the simulated leachate, where saponification rate, initial pH, initial concentration of Fe^{3+} , extraction time, phase ratio, and extraction temperature were 70%, 1.00, 12.25 g/L, 20 min, 1:1, and 298 K, respectively. Figure 6 shows that the iron extraction rate increased significantly with increased extractant concentration. With 0.2 mol/L D2EHPA, the Fe^{3+} extraction rate was only 26.58%. However, the Fe^{3+} extraction rate increased to 95.65% with 1.0 mol/L D2EHPA. As the extractant concentration was further increased to 1.3 mol/L and the iron extraction rate increased slightly. It has been shown that when the D2EHPA concentration exceeds 1 mol/L, difficulties in mass transfer occur due to the high viscosity of the organic extractant [21]. In order to reduce the amount of extractant used and avoid mass transfer difficulties, subsequent experiments used 1.0 mol/L D2EHPA.

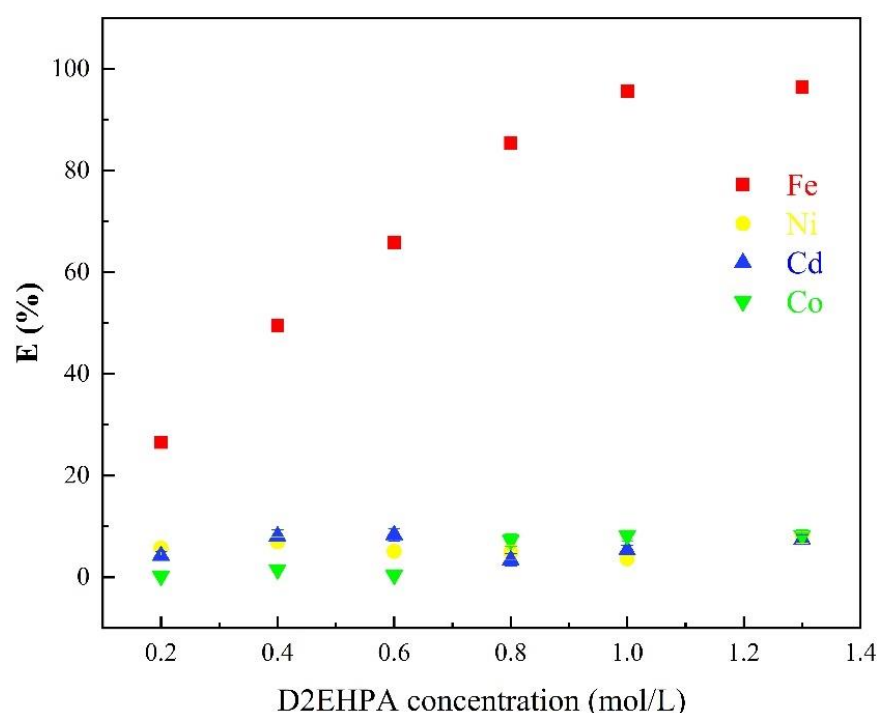


Figure 6. Effects of D2EHPA concentration under the conditions: room temperature (298 K), initial $[\text{Fe}^{3+}] = 12.25$ g/L, extraction time = 20 min, saponification rate = 70%, initial pH = 1.00, and phase ratio = 1:1.

3.1.6. Effects of the Phase Ratio on the Extraction

The impacts of the phase ratio on the Fe^{3+} extraction were studied by controlling the phase ratio of the saponified D2EHPA and Ni-Cd battery leachate at 0.2:1, 0.4:1, 0.6:1, 0.8:1, 1:1, and 1.3:1. The other conditions were the D2EHPA concentration of 1 mol/L, saponification rate of 70%, extraction time of 20 min, extraction temperature of 298 K, initial concentration of Fe^{3+} of 12.25 g/L, and initial pH of 1.00. From Figure 7, the Fe^{3+} extraction rate gradually increased with an increasing phase ratio. When the phase ratio was 0.2:1, the Fe^{3+} extraction was only 32.52%. With a 1:1 phase ratio, the Fe^{3+} extraction rate was 95.65%. Further increasing the phase ratio to 1.3:1, the Fe^{3+} extraction rate increased by only 3%. In order to reduce extractant consumption, the phase ratio was set to 1:1.

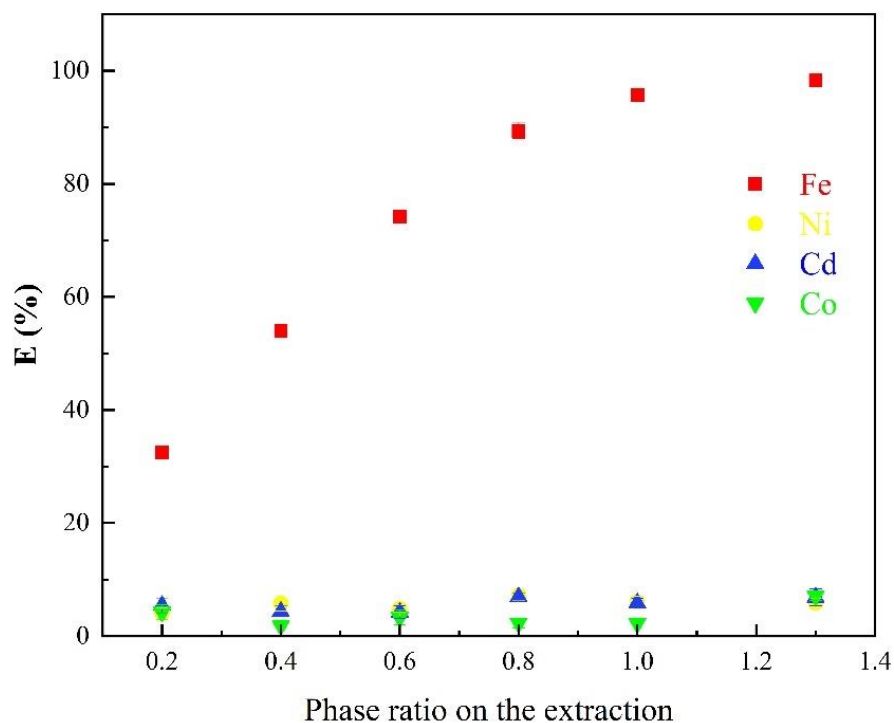


Figure 7. Effects of the phase ratio on the extraction under the conditions: room temperature (298 K), [D2EHPA] = 1 mol/L, initial [Fe³⁺] = 12.25 g/L, extraction time = 20 min, saponification rate = 70%, and initial pH = 1.00.

The McCabe-Thiele extraction equilibrium isotherms of Fe³⁺ were plotted based on the Fe³⁺ in the aqueous and organic phases under different phase ratios [22]. The concentration of Fe³⁺ in the raffinate after extraction was used as the X-axis, and the concentration of Fe³⁺ in loaded D2EHPA after extraction was used as the Y-axis. From Figure 8, with the work phase ratio of 1:1 on the extraction, the concentration of Fe³⁺ in the raffinate was less than 0.03 g/L after two theoretical extraction stages, while the iron’s extraction rate was more than 99%.

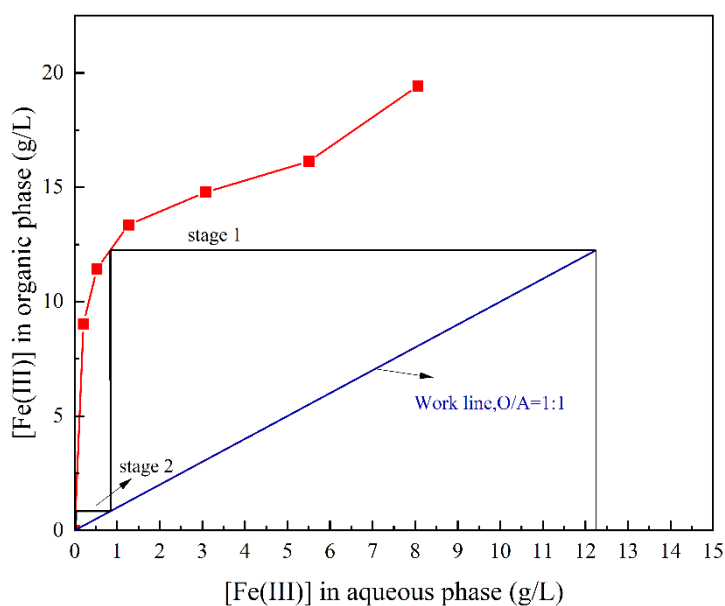
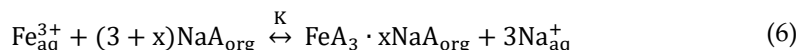


Figure 8. McCabe-Thiele extraction equilibrium isotherms of Fe³⁺ under the conditions: room temperature (298 K), [D2EHPA] = 1 mol/L, initial [Fe³⁺] = 12.25 g/L, extraction time = 20 min, saponification rate = 70%, and initial pH = 1.00.

3.2. Extraction Mechanism

3.2.1. Slope Analysis of the Extraction

When extractant D2EHPA was saponified with 10 mol/L NaOH, Na⁺ was loaded into the D2EHPA and replaced the H⁺ in the organic phase. Moreover, D2EHPA in the presence of dimers was depolymerized into monomers due to saponification [19]. The extraction equilibrium of iron can be supposed as follows:



where Fe_{aq}³⁺ is the iron ion in the leachate, A is the D2EHPA anion, NaA_{org} is the saponified D2EHPA, and Na_{aq}⁺ is the Na ion in the raffinate.

The extraction equilibrium constant K can be calculated as follows:

$$K = \frac{[\text{FeA}_3 \cdot x\text{NaA}]_{\text{org}} \cdot [\text{Na}^+]_{\text{aq}}^3}{[\text{Fe}^{3+}]_{\text{aq}} \cdot [\text{NaA}]_{\text{org}}^{(3+x)}} \quad (7)$$

where [FeA₃ · xNaA]_{org} is the iron concentration in the extracted D2EHPA, [Na⁺]_{aq} is the Na⁺ concentration in the raffinate, [Fe³⁺]_{aq} is the iron concentration in the raffinate after extraction, and [NaA]_{org} is the Na⁺ concentration in the loaded D2EHPA after extraction.

The distribution coefficient D_{Fe} is as follows:

$$D_{\text{Fe}} = \frac{[\text{Fe}^{3+}]_{\text{org}}}{[\text{Fe}^{3+}]_{\text{aq}}} = \frac{[\text{FeA}_3 \cdot x\text{NaA}]_{\text{org}}}{[\text{Fe}^{3+}]_{\text{aq}}} \quad (8)$$

where [Fe³⁺]_{org} is the iron concentration in the loaded D2EHPA after extraction and [Fe³⁺]_{aq} is the iron concentration in the raffinate after extraction.

Then, Equation (8) can be further derived as follows:

$$K = \frac{D_{\text{Fe}} \cdot [\text{Na}^+]_{\text{aq}}^3}{[\text{NaA}]_{\text{org}}^{(3+x)}} \quad (9)$$

Taking the logarithm of both sides of the Equation (9) at the same time:

$$\lg(D_{\text{Fe}} \cdot [\text{Na}^+]_{\text{aq}}^3) = \lg K + (3 + x)\lg [\text{NaA}]_{\text{org}} \quad (10)$$

The saponified D2EHPA, with concentrations varying from 0.2 mol/L to 1.3 mol/L, was used to extract the Fe³⁺ from the simulated leachate. The concentration of Fe³⁺ ([Fe³⁺]_{aq}) and Na⁺ ([Na⁺]_{aq}) in the raffinate can be directly determined with the instrument method. Meanwhile, the concentration of Fe³⁺ ([Fe³⁺]_{aq}) in the loaded organic phase can be calculated by mass balance. Therefore, D_{Fe} can be calculated by Equation (8). The relevant data was plotted in Figure 9a. The logarithm of D_{Fe} · [Na⁺]_{aq}³ was used as the Y-axis, and the logarithm of the concentration of the saponified D2EHPA was used as the X-axis.

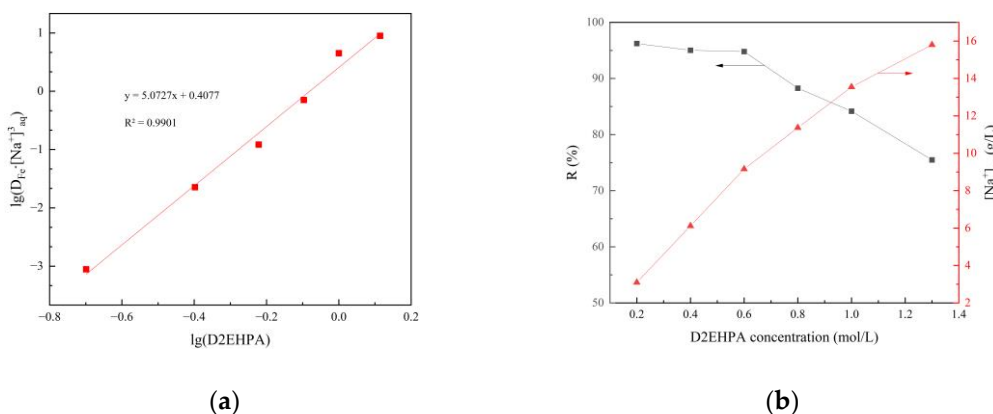


Figure 9. (a) Slope analysis of the extraction under various D2EHPA concentration, (b) Na⁺ replacement after extraction under various D2EHPA concentration.

The slope of the fitting line in Figure 9a is 5.07, which means the value of $(3 + x)$ was nearly 5. The results indicate that five molecules of D2EHPA were combined with one molecule of Fe^{3+} in the extraction process.

The replacement ratio of Na^+ loaded in saponified D2EHPA (R) before and after extraction can be calculated as follows:

$$R = \frac{[\text{Na}^+]_{\text{aq}}}{[\text{NaA}]_{\text{org}}} = \frac{[\text{Na}^+]_{\text{aq}}}{[\text{D2EHPA}] \cdot S_A} \quad (11)$$

where $[\text{Na}^+]_{\text{aq}}$ is the concentration of Na^+ in the raffinate after extraction, $[\text{NaA}]_{\text{org}}$ is the concentration of Na^+ loaded in saponified D2EHPA before extraction, $[\text{D2EHPA}]$ is the concentration of extractant D2EHPA, and S_A is the saponification of the extractant.

From Figure 9b, the replacement ratio of Na^+ was more than 80% with a D2EHPA concentration below 1.0 mol/L, which indicated most of the Na^+ in the organic phase was replaced by Fe^{3+} .

3.2.2. FT-IR Analysis of the D2EHPA after Extraction

Figure 10 shows that untreated D2EHPA, saponified D2EHPA, extracted D2EHPA, and stripped D2EHPA all display the characteristic absorption peak of $-\text{CH}_3$ (2956 cm^{-1}) and $-\text{CH}_2$ (2921 and 2853 cm^{-1}) [19]. From Figure 10a, the untreated D2EHPA shows characteristic peaks of $\text{P}=\text{O}$ group (1225 cm^{-1}) and $\text{P}-\text{O}-\text{H}$ group (1683 cm^{-1} and 1030 cm^{-1}) [19,23]. After saponification, water characteristic peaks appeared at 3402 cm^{-1} and 1642 cm^{-1} , and the characteristic $\text{P}-\text{O}-\text{H}$ peak moves from 1030 cm^{-1} to 1084 cm^{-1} , indicating that Na^+ replaced the H^+ in the $\text{P}-\text{O}-\text{H}$ group (Figure 10b). This shift also means that the D2EHPA in the presence of dimers was depolymerized into monomers, which was similar to previous work [19]. Meanwhile, the strong $\text{P}=\text{O}$ absorption peak at 1225 cm^{-1} weakens and shifts to 1205 cm^{-1} . This indicates that the $\text{P}=\text{O}$ group reacted with sodium hydroxide, thereby reducing the strength of the $\text{P}=\text{O}$ absorbance [19].

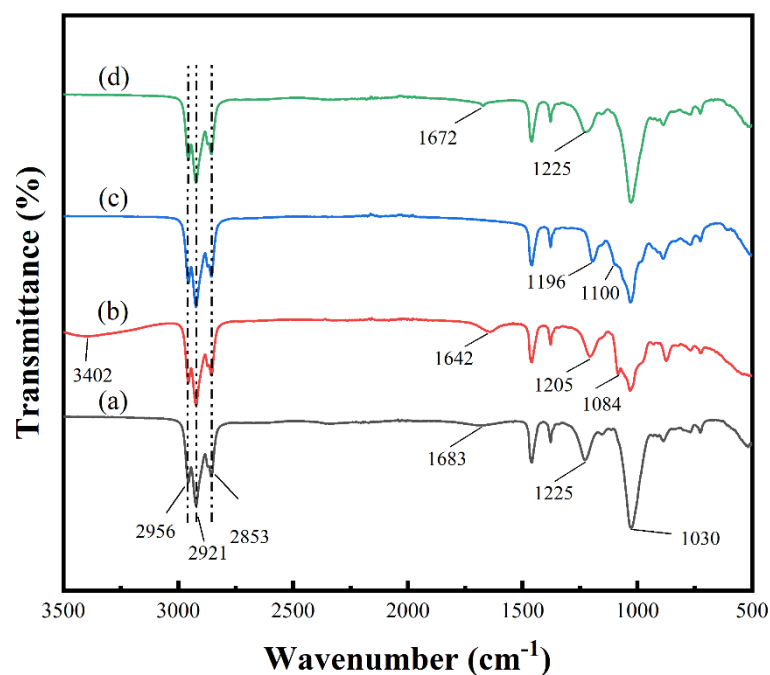


Figure 10. FT-IR spectra of (a) untreated D2EHPA, (b) saponified D2EHPA, (c) extracted D2EHPA, and (d) stripped D2EHPA. The extraction conditions: room temperature (298 K), $[\text{D2EHPA}] = 1 \text{ mol/L}$, initial $[\text{Fe}^{3+}] = 12.25 \text{ g/L}$, extraction time = 20 min, saponification rate = 70%, initial pH = 1.00, and phase ratio = 1:1. The stripping conditions: $[\text{oxalic acid}] = 1 \text{ mol/L}$, stripping time = 40 min, stripping temperature = 313 K, and phase ratio = 1:1.

After the extraction, the water peaks disappeared, indicating that most of the water in the organic phase was removed in the extraction process (Figure 10c). The P=O absorption peak at 1205 cm^{-1} shifts to 1196 cm^{-1} , indicating that the Fe^{3+} was loaded into the organic phase [19]. The results mean that the extraction mechanism of Fe^{3+} , using saponified D2EHPA, is also a cation exchange similar to the replacement of Na^+ for H^+ in the saponification process. The stripped D2EHPA spectrum was consistent with the untreated organic phase, while the P-O-H peak was observed again at 1683 cm^{-1} (Figure 10b). This indicates that most of the Fe^{3+} was stripped from the organic phase, which also verified the stripping effect of the oxalic acid.

3.3. Stripping of Loaded D2EHPA

3.3.1. Effects of Oxalic Acid Concentration on the Stripping

Figure 11 shows the Fe^{3+} stripping rate increases with increasing the oxalic acid concentration, while under the stripping temperature of 313 K, phase ratio of 1:1, and stripping time of 40 min. When the oxalic acid concentration was 1.0 mol/L, the Fe^{3+} stripping rate was 85.59%. The solubility of the oxalic acid was 90 g/L (nearly 1 mol/L) at 293 K, thus increasing the oxalic acid concentration above 1.0 mol/L may cause precipitation problems. In order to avoid oxalic acid precipitation, the oxalic acid concentration was set to 1.0 mol/L in the other stripping experiments.

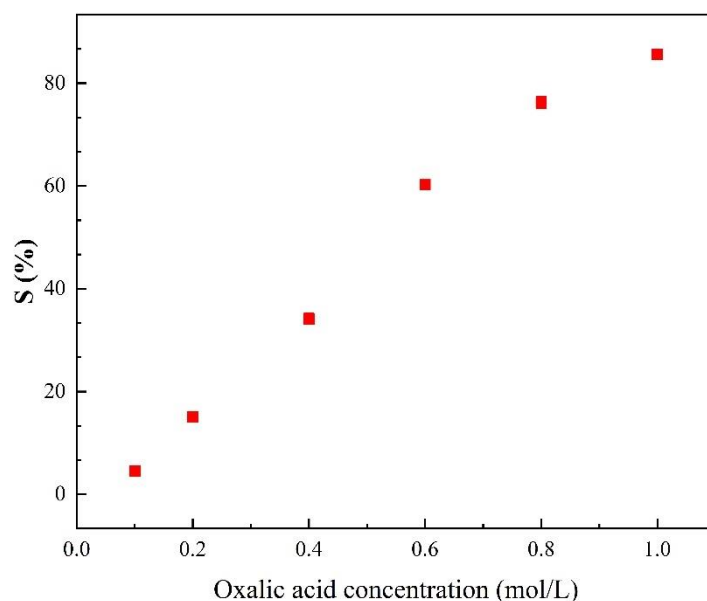


Figure 11. Effects of oxalic acid concentration on the stripping under the conditions: stripping time = 40 min, stripping temperature = 313 K, and phase ratio = 1:1.

3.3.2. Effects of Stripping Time

The effects of stripping time were investigated, where the concentration of the oxalic acid, stripping temperature, and phase ratio were 1 mol/L, 313 K, and 1:1, respectively. Figure 12 shows that the Fe^{3+} stripping rate increases with increasing the stripping time. When the stripping time was 5 min, the Fe^{3+} stripping efficiency was only 36.88%. As the stripping time increased to 40 min, the stripping efficiency rose to 86.21%. Further increases in the stripping time led to a slight increase in the stripping rate. In order to maximize the iron stripping efficiency, the stripping time should be 40 min.

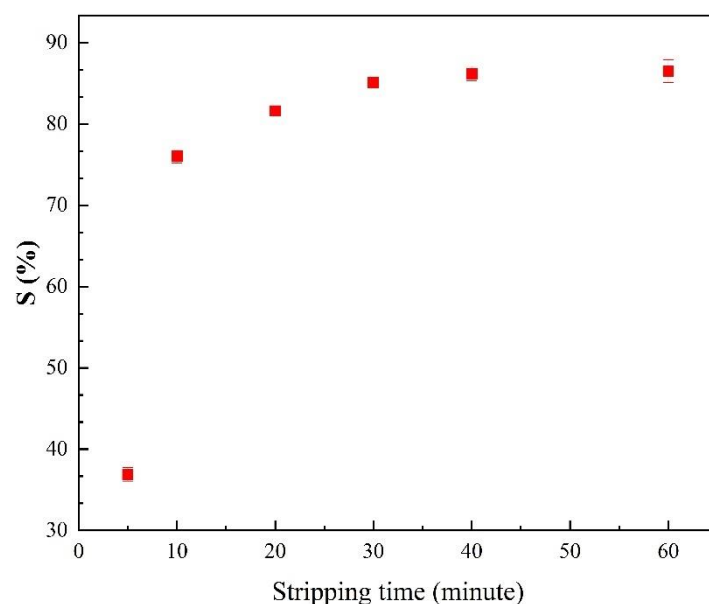


Figure 12. Effects of stripping time under the conditions: [oxalic acid] = 1 mol/L, stripping temperature = 313 K, and phase ratio = 1:1.

3.3.3. Effects of Stripping Temperature

The effects of the stripping temperature were investigated under these conditions, the concentration of oxalic acid of 1 mol/L, stripping time of 40 min, and phase ratio of 1:1. Figure 13 shows that increasing the stripping temperature facilitates Fe^{3+} stripping. At 298 K, the Fe^{3+} stripping rate was 68.37%. As the stripping temperature increased to 313 K, the Fe^{3+} stripping efficiency rose to 85.59%. Upon further increasing the stripping temperature, the Fe^{3+} stripping rate increased slowly. In order to ensure the maximum Fe^{3+} stripping rate and reduce the evaporative loss of the extractant, the optimal stripping temperature is 313 K.

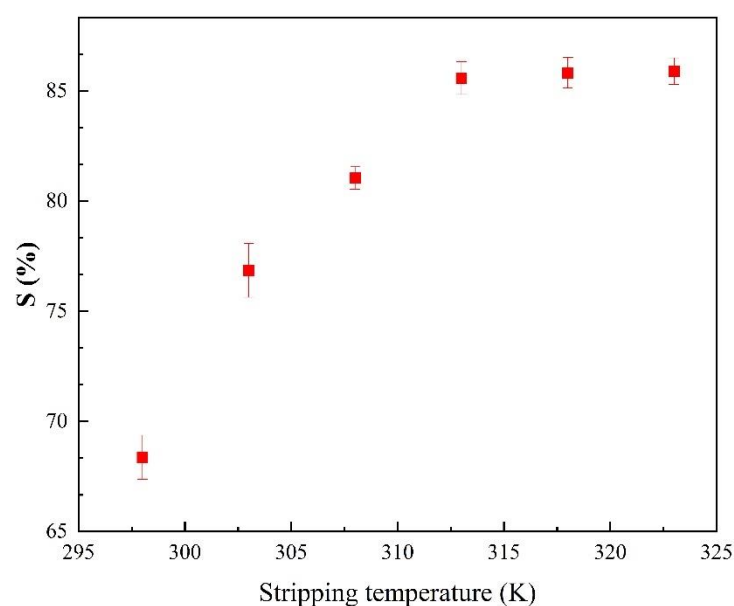


Figure 13. Effects of stripping temperature under the conditions: [oxalic acid] = 1 mol/L, stripping time = 40 min, and phase ratio = 1:1.

3.3.4. Effects of the Phase Ratio on the Stripping

The effects of the phase ratio on the stripping were investigated, while under the stripping temperature of 313 K, the concentration of oxalic acid of 1 mol/L, and a stripping time of 40 min. Figure 14 shows that as the phase ratio for stripping decreased, the Fe³⁺ stripping efficiency increased. With a phase ratio of 2:1, the stripping rate of Fe³⁺ was 48.77%. When the phase ratio changed to 1:1, the stripping rate increased to 85.96%. Further changing the phase ratio to 0.67:1, 0.33:1, 0.25:1, the Fe stripping efficiency increased to 91%, 92%, 92%, respectively. Considering the Fe³⁺ stripping efficiency, the optimum stripping phase ratio was set to 1:1.

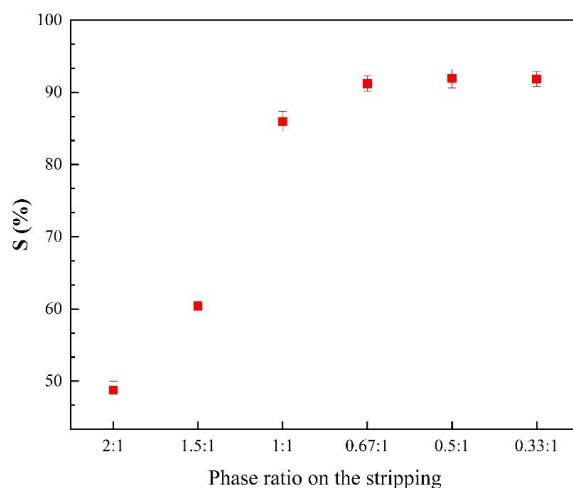


Figure 14. Effects of phase ratio on the stripping under the conditions: [oxalic acid] = 1 mol/L, stripping time = 40 min, and stripping temperature = 313 K.

The McCabe-Thiele stripping equilibrium isotherms of Fe³⁺ were drawn in Figure 15 based on the Fe³⁺ in the aqueous and organic phase under different phase ratios [24]. The concentration of Fe³⁺ in the organic phase after stripping was used as the X-axis, and the concentration of Fe³⁺ in stripping aqueous after stripping was used as the Y-axis. From Figure 15, with the work phase ratio of 1:1 on the stripping, the concentration of Fe³⁺ in the stripping aqueous was less than 0.18 g/L after two theoretical stripping stages, while iron's stripping rate was 95.6%.

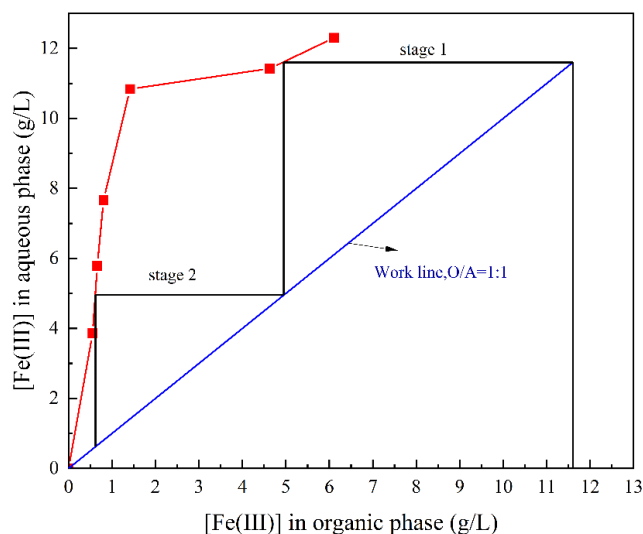


Figure 15. McCabe-Thiele stripping equilibrium isotherms of Fe³⁺ on the stripping under the conditions: [oxalic acid] = 1 mol/L, stripping time = 40 min, and stripping temperature = 313 K.

3.3.5. Stripping Experiment under the Optimal Conditions

The extracted D2EHPA was prepared under the optimal extraction conditions: room temperature (298 K), [D2EHPA] = 1 mol/L, extraction time = 20 min, saponification rate = 70%, initial pH = 1.00, and phase ratio = 1:1. Then, the organic phase loaded iron and other metals were stripped with oxalic acid under the conditions: [oxalic acid] = 1 mol/L, stripping time = 40 min, and stripping temperature = 313 K. The relevant stripping data were as Table 2. From Table 2, the concentration of iron in the stripping aqueous was 9.951 g/L, and the stripping rate of iron was 85.51% under the optimal stripping conditions. While the concentrations of Ni, Cd, and Co were only 0.011 g/L, 0.018 g/L, and 0.006 g/L, respectively. The results showed that most of the iron in the loaded organic phase was transferred into the stripping aqueous phase, and the concentrations of other metals were very low, which guaranteed the purity of the iron product.

Table 2. Stripping data under the optimal stripping conditions.

Elements	Metal Concentration in the Stripping		Metal Stripping Rate
	Aqueous (g/L)		
Fe	9.951		85.51%
Ni	0.011		0.85%
Cd	0.018		3.53%
Co	0.006		28.93%

4. Conclusions

The difficulties in the separation and recovery of iron from the leachate of spent Ni-Cd batteries are well known. This work provides a process for the separation of iron from spent Ni-Cd battery sulfuric acid leachate and its subsequent recovery. The iron is extracted with the saponified D2EHPA and then stripped with oxalic acid to obtain the high-value product, iron oxalate. After optimization, the single-stage extraction efficiency of iron was above 95% when the concentration of D2EHPA = 1 mol/L, saponification rate = 70%, extraction time = 20 min, initial pH = 1.00, phase ratio = 1:1, and extraction temperature = 298 K. The single-stage iron stripping rate using oxalic acid was above 85% when the concentration of oxalic acid = 1 mol/L, stripping temperature = 313 K, phase ratio = 1:1, and stripping time = 40 min. Moreover, the iron's extraction rate was more than 99% after two theoretical extraction stages, and the stripping rate was 95.6% after two theoretical stripping stages. The slope analysis indicates that five molecules of D2EHPA were combined with one molecule of Fe³⁺ in the extraction of Fe³⁺ using D2EHPA. The FT-IR analysis shows that the extraction mechanism of Fe³⁺ using the saponified D2EHPA is a cation exchange. This work provides the maximum recovery of high-value iron oxalate while allowing the continued treatment of the spent Ni-Cd battery waste stream.

Author Contributions: Conceptualization, L.Z. (Lei Zhou); Funding acquisition, Y.Z.; Investigation, L.Z. (Lei Zhou); Methodology, L.Z. (Lei Zhou) and Y.Z.; Resources, Y.Z.; Software, L.Z. (Lei Zhou), L.Z. (Lijin Zhang) and X.W.; Supervision, Y.Z. and R.J.; Validation, Y.Z.; Writing—original draft, L.Z. (Lei Zhou); Writing—review & editing, Y.Z., L.W., L.Z. (Lijin Zhang), X.W. and R.J. All authors have read and agreed to the published version of the manuscript.

Funding: This work was financially supported by the National Key Research and Development Program of China (2016YFC0400708) and the Natural Science Foundation of Guangdong Province, China (2023A1515012378).

Data Availability Statement: Data is contained within the article.

Conflicts of Interest: The authors declare that they have no known competing financial interests or personal relationships that could have appeared to influence the work reported in this paper.

References

1. Assefi, M.; Maroufi, S.; Yamauchi, Y.; Sahajwalla, V. Pyrometallurgical recycling of Li-ion, Ni–Cd and Ni–MH batteries: A minireview. *Curr. Opin. Green Sustain. Chem.* **2020**, *24*, 26–31. <https://doi.org/10.1016/j.cogsc.2020.01.005>.
2. Blumbergs, E.; Serga, V.; Platacis, E.; Maiorov, M.; Shishkin, A. Cadmium Recovery from Spent Ni–Cd Batteries: A Brief Review. *Metals* **2021**, *11*, 1714. <https://doi.org/10.3390/met11111714>.
3. Guo, X.; Song, Y.; Nan, J. Flow evaluation of the leaching hazardous materials from spent nickel-cadmium batteries discarded in different water surroundings. *Environ. Sci. Pollut. Res. Int.* **2018**, *25*, 5514–5520. <https://doi.org/10.1007/s11356-017-0923-0>.
4. Abidli, A.; Huang, Y.; Ben Rejeb, Z.; Zaoui, A.; Park, C.B. Sustainable and efficient technologies for removal and recovery of toxic and valuable metals from wastewater: Recent progress, challenges, and future perspectives. *Chemosphere* **2022**, *292*, 133102. <https://doi.org/10.1016/j.chemosphere.2021.133102>.
5. Wang, J.; Zhang, Y.; Yu, L.; Cui, K.; Fu, T.; Mao, H. Effective separation and recovery of valuable metals from waste Ni-based batteries: A comprehensive review. *Chem. Eng. J.* **2022**, *439*, 135767. <https://doi.org/10.1016/j.cej.2022.135767>.
6. Zhang, X.; Li, L.; Fan, E.; Xue, Q.; Bian, Y.; Wu, F.; Chen, R. Toward sustainable and systematic recycling of spent rechargeable batteries. *Chem. Soc. Rev.* **2018**, *47*, 7239–7302. <https://doi.org/10.1039/c8cs00297e>.
7. Randhawa, N.S.; Gharami, K.; Kumar, M. Leaching kinetics of spent nickel–cadmium battery in sulphuric acid. *Hydrometallurgy* **2016**, *165*, 191–198. <https://doi.org/10.1016/j.hydromet.2015.09.011>.
8. Fernandes, A.; Afonso, J.C.; Bourdot Dutra, A.J. Hydrometallurgical route to recover nickel, cobalt and cadmium from spent Ni–Cd batteries. *J. Power Sources* **2012**, *220*, 286–291. <https://doi.org/10.1016/j.jpowsour.2012.08.011>.
9. Agrawal, A.; Kumari, S.; Sahu, K.K. Iron and Copper Recovery/Removal from Industrial Wastes: A Review. *Ind. Eng. Chem. Res.* **2009**, *48*, 6145–6161. <https://doi.org/10.1021/ie900135u>.
10. El-Asmy, A.A.; Serag, H.M.; Mahdy, M.A.; Amin, M.I. Purification of phosphoric acid by minimizing iron, copper, cadmium and fluoride. *Sep. Purif. Technol.* **2008**, *61*, 287–292. <https://doi.org/10.1016/j.seppur.2007.11.004>.
11. Vinco, J.H.; Botelho Junior, A.B.; Duarte, H.A.; Espinosa, D.C.R.; Tenório, J.A.S. Purification of an iron contaminated vanadium solution through ion exchange resins. *Miner. Eng.* **2022**, *176*, 107337. <https://doi.org/10.1016/j.mineng.2021.107337>.
12. Xu, C.; Li, L.; Zhang, M.; Meng, X.; Peng, X.; Zeb, S.; Lu, Y.; Qiao, D.; Cui, Y.; Sun, G. Removal of Fe(III) from sulfuric acid leaching solution of phosphate ores with bisphosphonic acids. *Hydrometallurgy* **2022**, *208*, 105799. <https://doi.org/10.1016/j.hydromet.2021.105799>.
13. Hu, G.; Wu, Y.; Chen, D.; Wang, Y.; Qi, T.; Wang, L. Selective removal of iron(III) from highly salted chloride acidic solutions by solvent extraction using di(2-ethylhexyl) phosphate. *Front. Chem. Sci. Eng.* **2020**, *15*, 528–537. <https://doi.org/10.1007/s11705-020-1955-4>.
14. Wang, L.; Wang, Y.; Cui, L.; Gao, J.; Guo, Y.; Cheng, F. A sustainable approach for advanced removal of iron from CFA sulfuric acid leach liquor by solvent extraction with P507. *Sep. Purif. Technol.* **2020**, *251*, 117371. <https://doi.org/10.1016/j.seppur.2020.117371>.
15. Ma, H.-R.; Li, H.; Wu, W.; Qiao, X.-R. Separation of Fe(III) and Cr(III) from tannery sludge bioleachate using organophosphorus acid extractants. *Res. Chem. Intermed.* **2016**, *43*, 2333–2350. <https://doi.org/10.1007/s11164-016-2764-8>.
16. Yi, X.; Huo, G.; Tang, W. Removal of Fe(III) from Ni–Co–Fe chloride solutions using solvent extraction with TBP. *Hydrometallurgy* **2020**, *192*, 105265. <https://doi.org/10.1016/j.hydromet.2020.105265>.
17. Pavón, S.; Haneklaus, N.; Meerbach, K.; Bertau, M. Iron(III) removal and rare earth element recovery from a synthetic wet phosphoric acid solution using solvent extraction. *Miner. Eng.* **2022**, *182*, 107569. <https://doi.org/10.1016/j.mineng.2022.107569>.
18. Lupi, C.; Piloni, D. Effectiveness of saponified D2EHPA in Zn(II) selective extraction from concentrated sulphuric solutions. *Miner. Eng.* **2020**, *150*, 106278. <https://doi.org/10.1016/j.mineng.2020.106278>.
19. Song, Y.; Zhao, Z.; He, L. Lithium recovery from Li₃PO₄ leaching liquor: Solvent extraction mechanism of saponified D2EHPA system. *Sep. Purif. Technol.* **2020**, *249*, 117161. <https://doi.org/10.1016/j.seppur.2020.117161>.
20. Song, Y.; He, L.; Zhao, Z.; Liu, X. Separation and recovery of lithium from Li₃PO₄ leaching liquor using solvent extraction with saponified D2EHPA. *Sep. Purif. Technol.* **2019**, *229*, 115823. <https://doi.org/10.1016/j.seppur.2019.115823>.
21. Nogueira, C.A.; Delmas, F. New flowsheet for the recovery of cadmium, cobalt and nickel from spent Ni–Cd batteries by solvent extraction. *Hydrometallurgy* **1999**, *52*, 267–287. [https://doi.org/10.1016/s0304-386x\(99\)00026-2](https://doi.org/10.1016/s0304-386x(99)00026-2).
22. Kim, H.-I.; Moon, G.; Choi, I.; Lee, J.-Y.; Jyothi, R.K. Hydrometallurgical process development for the extraction, separation and recovery of vanadium from spent desulfurization catalyst bio-leach liquors. *J. Clean. Prod.* **2018**, *187*, 449–458. <https://doi.org/10.1016/j.jclepro.2018.03.247>.
23. Jin, Y.; Ma, Y.; Weng, Y.; Jia, X.; Li, J. Solvent extraction of Fe³⁺ from the hydrochloric acid route phosphoric acid by D2EHPA in kerosene. *J. Ind. Eng. Chem.* **2014**, *20*, 3446–3452. <https://doi.org/10.1016/j.jiec.2013.12.033>.
24. Belhadj, N.; Benabdallah, T.; Coll, M.T.; Fortuny, A.; Hadj Youcef, M.; Sastre, A.M. Counter-current separation of cobalt(II)–nickel(II) from aqueous sulphate media with a mixture of Primene JMT–Versatic 10 diluted in kerosene. *Sep. Sci. Technol.* **2019**, *55*, 513–522. <https://doi.org/10.1080/01496395.2019.1577271>.

Disclaimer/Publisher’s Note: The statements, opinions and data contained in all publications are solely those of the individual author(s) and contributor(s) and not of MDPI and/or the editor(s). MDPI and/or the editor(s) disclaim responsibility for any injury to people or property resulting from any ideas, methods, instructions or products referred to in the content.